
Similarity Field Theory: A General Mathematical Framework for Intelligence

Kei-Sing Ng
 max.ksng.contact@gmail.com

Abstract

We posit that persisting and transforming similarity relations form the structural basis of any comprehensible dynamic system. This paper introduces **Similarity Field Theory**, a mathematical framework that formalizes the principles governing similarity values among entities and their evolution. We define: (1) a *similarity field* $S : U \times U \rightarrow [0, 1]$ over a universe of entities U , satisfying reflexivity $S(E, E) = 1$ and treated as a *directed relational field* (asymmetry and non-transitivity are allowed); (2) the evolution of a system through a sequence $Z_p = (X_p, S^{(p)})$ indexed by $p = 0, 1, 2, \dots$; (3) concepts K as entities that induce **fibres** $F_\alpha(K) = \{E \in U \mid S(E, K) \geq \alpha\}$, i.e., superlevel sets of the unary map $S_K(E) := S(E, K)$; and (4) a generative operator G that produces new entities. Within this framework, we formalize a generative definition of intelligence: an operator G is intelligent with respect to a concept K if, given a system containing entities belonging to the fibre of K , it generates new entities that also belong to that fibre. Similarity Field Theory thus offers a foundational language for characterizing, comparing, and constructing intelligent systems. We prove two theorems: (i) asymmetry blocks mutual inclusion; and (ii) stability requires either an anchor coordinate or eventual confinement within a level set. These results ensure that the evolution of similarity fields is both constrained and interpretable, culminating in an exploration of how the framework allows us to interpret large language models and present empirical results using large language models as experimental probes of societal cognition.

1 Introduction

We may regard the world as an evolving system. Within this system, similarity relations exist; without them, everything would collapse into undifferentiated chaos and the world we comprehend would cease to exist. Consider a cup before you: one second later it remains recognizably as a cup because certain similarities persist. If the cup falls and shatters, some similarities diminish while some others remain. These persisting and changing similarities jointly constitute the world we comprehend.

This paper formalizes this intuition by proposing a mathematical framework, **Similarity Field Theory**. Just as classical mechanics relies on calculus to analyze the continuous variation of physical quantities, Similarity Field Theory provides the essential constructs to analyze how intelligent systems preserve, modify, and generate similarity structures. We begin by establishing our foundational constructs—entities, concepts, and a similarity field. We then describe system evolution via a sequence $Z_p = (X_p, S^{(p)})$ and introduce a generative operator, culminating in a formal, operational definition of intelligence as the capacity to preserve conceptual structure under generation.

Contributions. To support rapid assessment by reviewers, we summarize core contributions.

- A first-principles framework that treats graded, possibly asymmetric similarity as the primitive substrate for cognition and intelligence, with fibres as superlevel sets that define conceptual membership.
- A sequence-based evolution formalism, including a strengthened stability theorem that characterizes anchors versus eventual confinement and an incompatibility theorem showing how asymmetry forbids reciprocal inclusion under self-set thresholds.
- An operational, generative definition of intelligence in terms of fibre preservation and coverage/fidelity measures, applicable across models and modalities.
- A program for interpretability that views networks as compositions of calibrated similarity fields and demonstrates how pairwise typicality probes recover aggregate cognitive structure.

2 Related Work

Similarity Field Theory builds upon and extends several foundational areas. We position it as a first-principles framework that elevates similarity to a primitive substrate, complementing and unifying existing concepts rather than deriving from any single field.

2.1 Fuzzy Set Theory: A Formal Analogy and an Essential Distinction

A core structure in our framework—a grouping of entities based on their similarity to a given concept—is formally analogous to the ‘ α -cut’ in Zadeh’s Fuzzy Set Theory [2]. This formal link provides a useful bridge to a mature field. However, this similarity is formal rather than foundational. The primary goal of Fuzzy Set Theory is to represent static knowledge under conditions of vagueness. In contrast, the central aim of Similarity Field Theory is to formulate a theory of intelligence based on the *dynamics* of how conceptual structures evolve and are generated, which can reuse fuzzy constructs when convenient, without being reducible to them. Our fundamental primitive is the similarity relation itself, modeled as a directed field S . Our framework is therefore not an extension of Fuzzy Set Theory but a relation-centric dynamic similarity theory.

2.2 Metric Spaces: Relaxed Axioms for Cognitive Modeling

Our framework deliberately departs from the rigid axioms of metric spaces. The requirement for a distance function to be symmetric and to obey the triangle inequality, while essential for describing physical space, is often too restrictive for modeling the nuances of cognitive or conceptual space. In practice, machine learning routinely employs measures such as cosine similarity, KL divergence, Jensen–Shannon divergence, and general Bregman divergences; several of these are asymmetric and/or violate the triangle inequality, motivating a relaxation of metric axioms for conceptual geometry [12, 7, 8, 9, 10, 11, 3]. For the following examples, we fix a single similarity notion S over the shared universe U (e.g., cosine in a common embedding space or a corpus-based associative measure); all pairwise comparisons refer to this same S . Consider *lion* (A), *domestic cat* (B), and *household pet* (C): $S(A, B)$ is high (both are felids), $S(B, C)$ is high (cats are prototypical pets), yet $S(A, C)$ is much lower (lions are not household pets), yielding high $S(A, B)$ and $S(B, C)$ but comparatively low $S(A, C)$.

2.3 Category Theory: A Language of Structure

Category theory provides a language for abstract structures, describing objects and their connections (morphisms). In the standard view, the link between two objects is a discrete, binary matter: a morphism either exists or does not. While powerful, this is insufficient to capture the graded nature of conceptual relations. We use a similarity field S taking values in $[0, 1]$ to quantify the strength of belonging/connection; given a concept K , we express structure and invariants via threshold sets of $S(\cdot, K)$; generation is “intelligent” iff it preserves and expands these threshold sets along the evolution. We do not read S as a discrete morphism between arbitrary objects; instead, we center on the concept K and study $S(\cdot, K)$ and its fibres $F_\alpha(K)$, using strength rather than mere existence to characterize belonging and connection. More importantly, this framework targets any system organized by similarity—from perception and learning to machine models, social bargaining, and

institutional design—rather than being confined to categorical settings or specialist uses of “fibre”. Enriched categorical phrasing is only an explanatory lens; our theory and results hold even without adopting it [13, 14].

2.4 A Theoretical Foundation for Model Interpretability

2.4.1 Current Explorations and the Need for a Theory

The academic community has made explorations into model interpretability, developing techniques to trace information “circuits” [21], identify “persona vectors” in activation space [25, 26], and perform “representation engineering” [24, 22, 23]. These empirical works enhance our ability to inspect AI systems, but they often lack a unifying mathematical theory that explains how these observed structures emerge from first principles. The Similarity Field Theory framework is proposed not to replace these techniques, but to offer a foundational mathematical perspective, based on how similarity relations constitute concepts, to help unify and guide these interpretability studies at a deeper, structural level.

2.4.2 Beyond a Purely Statistical View

Viewing a neural network as a statistical learning machine is a dominant and effective practice; it excels at characterizing in-distribution input–output behavior but offers limited insight into the formation of internal conceptual structure and into out-of-distribution (OOD) phenomena. Similarity Field Theory complements this view from the angle of conceptual similarity: we regard a trained model as a complex system composed of nested similarity fields and restate interpretability as a task of conceptual deconstruction—identifying latent concepts formed inside the model and defining them via their fibres (the sets of inputs that elicit high similarity responses). Consequently, the research goal shifts from merely fitting external statistics to understanding and organizing these concept fibres, enabling structured judgments beyond the training distribution in accordance with conceptual similarity rather than being constrained by frequency statistics of the training distribution. For example, if the training data include only “red circles” and “green triangles” and never “green circles,” the model can still classify a green circle as a circle because it matches along the fibre of the concept “circle,” rather than relying on frequency co-occurrence.

3 Foundational Constructs

Definition 1 (Entity). An *entity*, denoted E , is any identifiable element of discourse. An entity can be atomic, a concept, or itself a similarity relation.

Definition 2 (Universe). The *universe*, denoted U , is the set of all entities.

Definition 3 (Concept). A *concept*, denoted K , is an entity that serves as a representation for a class of other entities. It induces a unary map $S_K(E) := S(E, K)$ and thereby defines fibres as its superlevel sets.

Definition 4 (Similarity Field). A *similarity field* is a mapping $S : U \times U \rightarrow [0, 1]$ satisfying reflexivity: $S(E, E) = 1$ for all $E \in U$. We treat S as a *directed relational field*; symmetry and transitivity are not assumed.

Definition 5 (Fibre). Given a concept $K \in U$ and a threshold $\alpha \in [0, 1]$, the *fibre* induced by K is the superlevel set:

$$F_\alpha(K) = \{E \in U \mid S(E, K) \geq \alpha\}.$$

Proposition 1 (Fibre monotonicity). Fix $K \in U$. If $\alpha \geq \beta$, then $F_\alpha(K) \subseteq F_\beta(K)$.

Proof. If $E \in F_\alpha(K)$, then $S(E, K) \geq \alpha \geq \beta$, hence $E \in F_\beta(K)$. \square

Proposition 2 (Intersection identity). For fixed $K \in U$ and thresholds $\{\alpha_r\}_{r=1}^m$, we have $\bigcap_{r=1}^m F_{\alpha_r}(K) = F_{\max_r \alpha_r}(K)$.

Proof. If $E \in \bigcap_{r=1}^m F_{\alpha_r}(K)$, then $S(E, K) \geq \alpha_r$ for all r , so $S(E, K) \geq \max_r \alpha_r$ and $E \in F_{\max_r \alpha_r}(K)$. The reverse inclusion is immediate. \square

Structural assumptions (minimal). We work with the weakest topological or graph structures needed : a domain of observables $D \subseteq [0, 1]^n$ admits well-defined limits and closures (e.g., by restricting to compact subsets), so that sequence limits, ω -limit sets, and level sets are well-defined. Smoothness is assumed only when explicitly required.

Terminology clarification. Throughout, “field” means a value-assigning function in the geometric sense; it is neither an algebraic field nor a physical field theory.

3.1 On the Nature of the Similarity Field

It is a crucial feature of our framework that the similarity field S is defined broadly, requiring only reflexivity. We deliberately do not enforce two stronger conditions common in classical mathematics:

- **Symmetry:** We do not assume that $S(E_1, E_2) = S(E_2, E_1)$. This allows the framework to model asymmetric cognitive phenomena in reality, such as the perceived similarity of a novice to an expert, which is typically higher than the reverse.
- **Transitivity:** High similarity need not be transitive, aligning with many cognitive examples.

This deliberate relaxation is motivated by the arguments presented in Section 2, distinguishing Similarity Field Theory from frameworks based on *Metric Spaces* or strict *Equivalence Relations*. While a field satisfying all three properties is a valid special case, our broader definition is essential for modeling the continuous and overlapping nature of conceptual structures in the real world.

3.2 Properties of Similarity Fields

The properties of the similarity field, particularly its allowance for asymmetry, give rise to non-trivial principles governing conceptual membership. We formalize some of these properties below.

Proposition 3. *If S is a similarity field, $d = 1 - S$ is not.*

Proof. For d to be a similarity field, it must satisfy $d(E, E) = 1$. By definition, $d(E, E) = 1 - S(E, E) = 1 - 1 = 0$. This implies the contradiction $0 = 1$. \square

Proposition 4 (Closure under Multiplication). *If S_1, S_2 are similarity fields, so is their pointwise product $S_1 \cdot S_2$.*

Proof. The range remains $[0, 1]$. For reflexivity, $(S_1 \cdot S_2)(E, E) = S_1(E, E) \cdot S_2(E, E) = 1 \cdot 1 = 1$. \square

Proposition 5 (Closure under Convex Combination). *If $\{S_k\}$ is a collection of similarity fields and $\{w_k\}$ are non-negative weights summing to 1, then $\sum w_k S_k$ is a similarity field.*

Proof. The range remains $[0, 1]$. For reflexivity, $(\sum w_k S_k)(E, E) = \sum w_k S_k(E, E) = \sum w_k \cdot 1 = 1$. \square

Theorem 1 (Incompatibility Theorem). *Given two distinct entities $E_1, E_2 \in U$. Let their similarity values be $x = S(E_1, E_2)$ and $y = S(E_2, E_1)$, produced by the single similarity field S . If $x \neq y$ (i.e., the similarity relation is asymmetric), then the following two conditions cannot both be true simultaneously:*

1. *E_1 belongs to the fibre induced by E_2 as a concept, with threshold y (i.e., $E_1 \in F_y(E_2)$).*
2. *E_2 belongs to the fibre induced by E_1 as a concept, with threshold x (i.e., $E_2 \in F_x(E_1)$).*

Proof. We use proof by contradiction. Assume that both condition 1 and condition 2 are simultaneously true.

- From condition 1 being true, by the definition of a fibre $F_y(E_2) = \{E \in U \mid S(E, E_2) \geq y\}$, we must have $S(E_1, E_2) \geq y$. Substituting $x = S(E_1, E_2)$, we get $x \geq y$.

- From condition 2 being true, by the definition of a fibre $F_x(E_1) = \{E \in U \mid S(E, E_1) \geq x\}$, we must have $S(E_2, E_1) \geq x$. Substituting $y = S(E_2, E_1)$, we get $y \geq x$.

Combining these two results, we have $x \geq y$ and $y \geq x$, which necessarily implies $x = y$. However, this contradicts the theorem's premise that $x \neq y$. Therefore, our initial assumption is false, meaning that condition 1 and condition 2 cannot both be true simultaneously. \square

Significance of Theorem 1: It is precisely the introduction of asymmetry that makes this theorem a fundamental and non-trivial principle. Far from being a mere restatement of definitions, it reveals the inherent limitations and forced imbalance that conceptual membership inevitably faces in an asymmetric world. **It establishes the impossibility of reciprocal inclusion: if E_1 's perspective on E_2 differs from E_2 's perspective on E_1 (i.e., $x \neq y$), then they cannot simultaneously be members of each other's conceptual fibres when the threshold for inclusion is set by the other's standard.** Thus, this theorem provides a formal explanation for negotiation deadlocks in social interaction: when two parties' assessments of each other's positions are asymmetric, and both adopt the other's standard as the threshold for acceptance, a mutual agreement becomes mathematically impossible unless one or both parties adjust their acceptance criteria (i.e., the fibre threshold).

This principle is illustrated by the Novice (N) and Expert (E) scenario. Suppose $S(N, E) = 0.9$ and $S(E, N) = 0.2$. The Novice may belong to the Expert's fibre ($N \in F_{0.2}(E)$ since $0.9 \geq 0.2$), but the theorem guarantees the impossibility of the reverse: the Expert cannot belong to the Novice's fibre at the Novice's standard ($E \notin F_{0.9}(N)$ since $0.2 < 0.9$). The asymmetry in similarity mathematically forbids a symmetric sense of belonging.

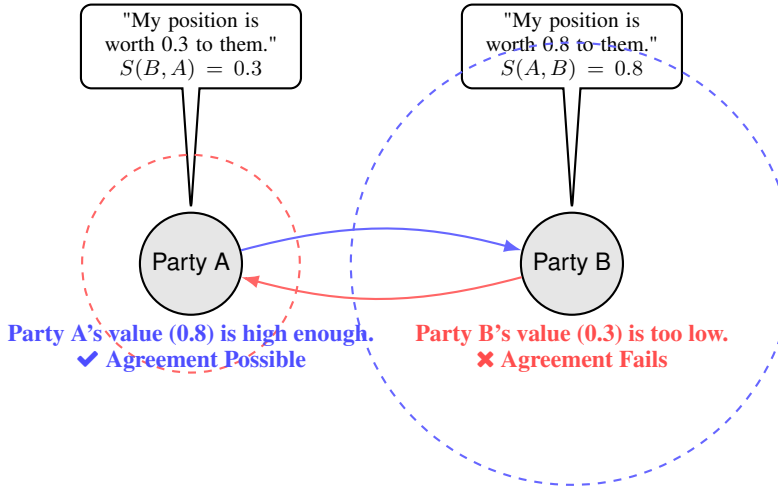


Figure 1: The Incompatibility Theorem visualized through a negotiation. Each party's "acceptance fibre" is defined by the other's perceived value. Party B's offer ($S(B, A) = 0.3$) is too low to enter Party A's acceptance fibre (threshold 0.8). Conversely, Party A's offer ($S(A, B) = 0.8$) easily clears Party B's threshold (0.3). Because the condition is not met for both, mutual agreement is impossible.

4 System Evolution via Sequences

Sequence-only stance. We do not introduce flow maps; all notions of evolution, stability, and ω -limits are expressed purely in terms of sequences.

Definition 6 (System-State Sequence). A *system-state sequence* is a sequence $Z_p = (X_p, S^{(p)})$ with $p = 0, 1, 2, \dots$, where $X_p \subseteq U$ is a finite set of entities and $S^{(p)} : U \times U \rightarrow [0, 1]$ is a similarity field at step p .

Index interpretation. The index p may denote discrete time, training steps/epochs, rounds of interaction, or any other well-ordered design parameter; our results depend only on its ordering, not on its physical interpretation. Even if an underlying continuous time exists, empirical measurements

are effectively discrete at finite resolution; accordingly, we adopt a sequence-based formalism while remaining compatible with continuous-time models where available.

The evolution of a system-state sequence can be characterized by two primary modes:

1. **Field Variation:** For a fixed set of entities, their relational structure changes along the sequence via $S^{(p)}(E_i, E_j)$. When p samples a continuous underlying parameter, differentiability of $S^{(p)}$ may be assumed only when needed.
2. **Discrete Composition Change:** The set X_p evolves via the addition/removal/modification of entities. This mode is driven by a generative operator (defined later).

Eventual confinement and absorbing sets. A subset $\mathcal{A} \subseteq U$ is called an absorbing set for a given evolution sequence if there exists p^* such that for all $p \geq p^*$, the entities under consideration lie in \mathcal{A} and never leave it along the subsequent sequence. When \mathcal{A} is a fibre $F_\alpha(K)$, we may say the sequence exhibits eventual confinement inside the fibre of concept K .

4.1 The Principle of Foundational Stability

Background and Core Significance. This theorem establishes, with mathematical rigor, a foundational principle of cognition that scales from the individual mind to the macro-society: any coherent, stable cognitive system is mathematically dependent on at least one long-term, foundational belief or concept that serves as a source of stability. Without a stability source, collapse is inevitable. In any system composed of interconnected elements, the stability of one property necessarily depends on the stability of its determinants.

Topological convention. We fix an embedding $D \subseteq [0, 1]^n$ and endow D with its subspace topology. Unless otherwise stated, closures \overline{A} appearing in C_c^* are taken in the ambient space $[0, 1]^n$. The ω -limit set collects cluster points in the ambient closure \overline{D} [43].

Set-up. Let $f : D \rightarrow [0, 1]$ be non-constant. For each index p , define the determining vector

$$\mathbf{v}_p = (S^{(p)}(E_1, E'_1), \dots, S^{(p)}(E_n, E'_n)) \in D, \quad y_p := f(\mathbf{v}_p).$$

A sequence y_p is called stable if there exists $c \in [0, 1]$ such that for every $\epsilon > 0$ there is p^* with $|y_p - c| \leq \epsilon$ for all $p \geq p^*$. For $c \in [0, 1]$ and $\epsilon > 0$, define the level-set tube $N_\epsilon(c) := \{x \in D : |f(x) - c| \leq \epsilon\}$ and the closed level set

$$C_c^* := \bigcap_{m=1}^{\infty} \overline{\{x \in D : |f(x) - c| \leq 1/m\}}.$$

The ω -limit set is $\omega(\mathbf{v}) := \{x \in \overline{D} : \exists p_k \rightarrow \infty \text{ with } \mathbf{v}_{p_k} \rightarrow x\}$. A coordinate sequence $\pi_i(\mathbf{v}_p)$ is called an anchor if it converges.

Theorem 2 (Stability Theorem, strengthened). *Assume $y_p = f(\mathbf{v}_p)$ is stable with limit c . Then:*

1. *For every $\epsilon > 0$ there exists p_ϵ such that $\mathbf{v}_p \in N_\epsilon(c)$ for all $p \geq p_\epsilon$. Hence $\omega(\mathbf{v}) \subseteq C_c^*$.*
2. *If f is continuous, then $\omega(\mathbf{v}) \subseteq f^{-1}(\{c\})$.*
3. *Either some coordinate $\pi_i(\mathbf{v}_p)$ converges, or $\omega(\mathbf{v})$ contains at least two distinct points and is contained in C_c^* .*

Lemma 1 (Separation Criterion). *Let $A, B \subseteq D$ and $\delta > 0$ be such that \mathbf{v}_p visits A and B infinitely often, and $|f(a) - f(b)| \geq \delta$ for all $a \in A, b \in B$. Then $y_p = f(\mathbf{v}_p)$ does not converge.*

Proof. Choose subsequences along visits to A and to B . Their images under f differ by at least δ , so $\limsup y_p - \liminf y_p \geq \delta > 0$, which rules out convergence. \square

Lemma 2. *If $\{\mathbf{v}_p\}$ has a unique cluster point x^* in the ambient compact space $[0, 1]^n$ (hence also in \overline{D}), then $\mathbf{v}_p \rightarrow x^*$, so each coordinate $\pi_i(\mathbf{v}_p)$ converges. Consequently, if no coordinate converges, then the set of ambient cluster points contains at least two distinct points.*

Proof. If $\mathbf{v}_p \not\rightarrow x^*$, there exist $\eta > 0$ and infinitely many p with $\|\mathbf{v}_p - x^*\| \geq \eta$. By compactness of $[0, 1]^n$, this subsequence has a convergent sub-subsequence with limit $y \neq x^*$, contradicting uniqueness. \square

Proof of Theorem 2. Let $y_p = f(\mathbf{v}_p)$ and assume $y_p \rightarrow c$. Then for every $\epsilon > 0$ there exists p_ϵ such that $|f(\mathbf{v}_p) - c| \leq \epsilon$ for all $p \geq p_\epsilon$, i.e., $\mathbf{v}_p \in N_\epsilon(c)$ eventually. Hence any cluster point x of $\{\mathbf{v}_p\}$ lies in every $\overline{N_{1/m}(c)}$, and thus $\omega(\mathbf{v}) \subseteq C_c^*$. If, in addition, f is continuous and $\mathbf{v}_{p_k} \rightarrow x \in \omega(\mathbf{v})$, then $f(x) = \lim_{k \rightarrow \infty} y_{p_k} = c$, so $\omega(\mathbf{v}) \subseteq f^{-1}(\{c\})$. For item (3), if some coordinate $\pi_i(\mathbf{v}_p)$ converges, we are in the first alternative of item (3). Otherwise, by Lemma 2, the ambient cluster set contains at least two distinct points, and by the first paragraph $\omega(\mathbf{v}) \subseteq C_c^*$, which is the second alternative of item (3). \square

Equivalent tail characterization. For sequences $y_p = f(\mathbf{v}_p)$, $y_p \rightarrow c$ if and only if for every $\epsilon > 0$ there exists p_ϵ such that $\mathbf{v}_p \in N_\epsilon(c)$ for all $p \geq p_\epsilon$.

Proof. If $y_p \rightarrow c$, then for every $\epsilon > 0$ there exists p_ϵ with $|f(\mathbf{v}_p) - c| \leq \epsilon$ for all $p \geq p_\epsilon$, hence $\mathbf{v}_p \in N_\epsilon(c)$. Conversely, if for every $\epsilon > 0$ there exists p_ϵ with $\mathbf{v}_p \in N_\epsilon(c)$ for all $p \geq p_\epsilon$, then $|f(\mathbf{v}_p) - c| \leq \epsilon$ for all large p , so $y_p \rightarrow c$. \square

Corollary 1 (Contrapositive Test). *If there exists $\epsilon_0 > 0$ such that $\mathbf{v}_p \notin N_{\epsilon_0}(c)$ for infinitely many p , then y_p cannot be stable at c .*

Sufficient tail condition. For every $\epsilon > 0$, if there exists p_ϵ with $\mathbf{v}_p \in N_\epsilon(c)$ for all $p \geq p_\epsilon$, then $y_p \rightarrow c$, and in particular $\omega(\mathbf{v}) \subseteq C_c^*$. In this sense, an absorbing set is any set that the sequence eventually enters and then remains in.

Proof. The assumption implies $|f(\mathbf{v}_p) - c| \leq \epsilon$ for all large p and every $\epsilon > 0$, hence $y_p \rightarrow c$. Any cluster point must lie in every $\overline{N_{1/m}(c)}$, so $\omega(\mathbf{v}) \subseteq C_c^*$. \square

Illustrative Examples. Mutual cancellation: for $f(v_1, v_2) = (v_1 + v_2)/2$ with $v_1(p) = 0.5 + 0.5 \sin p$ and $v_2(p) = 0.5 - 0.5 \sin p$, each coordinate oscillates but $f \equiv 0.5$ is perfectly stable. Saturation: for $f(x) = \sigma(w^\top x + b)$ with a bounded monotone activation σ , if $w^\top x + b$ remains in a saturated regime, then $f(x)$ is nearly constant despite input jitter.

5 Generative Dynamics and Intelligence

Definition 7 (Generative Operator). A *generative operator*, denoted G , is a function that maps a current set of entities to a new set:

$$E_{\text{new}} = G(X_p).$$

The system then undergoes discrete evolution according to the update rule $X_{p+1} = X_p \cup E_{\text{new}}$, yielding an updated pair $Z_{p+1} = (X_{p+1}, S^{(p+1)})$.

In physics, energy is the ability to do work. Analogously, our prior work [1] gave an informal definition of intelligence: “intelligence is the ability, given entities exemplifying a concept, to generate entities exemplifying the same concept.” This conceptual work is translated into the physical world by the action of a generative operator. For example, a large language model that, when given the conceptual requirement “a Python function to efficiently sort a list of numbers”, generates the correct and functional source code.

Within the Similarity Field Theory framework, this principle is expressed formally. The premise, “given entities exemplifying a concept,” corresponds to a system-state Z_p that contains a subset of entities $X_K \subseteq X_p$, where every entity in X_K belongs to a fibre $F_\alpha(K)$.

Intelligence with respect to a concept K is the capacity of a generative operator G to produce new entities $E' \in G(X_p)$ that also belong to the fibre $F_\alpha(K)$ by satisfying the condition:

$$S(E', K) \geq \alpha.$$

Example (ChatGPT, Ghibli style). Let K denote the concept “Studio Ghibli–style image.” Provide a reference context of Ghibli-style images and prompt ChatGPT to produce new frames under the same context. Using a fixed similarity function $S(\cdot, K)$ (e.g., style embeddings or calibrated ratings) to score each output, if a substantial portion of the outputs satisfy $S \geq \alpha$ (high coverage) and the average score is high (high fidelity), then ChatGPT is α -intelligent with respect to the concept “Ghibli-style image.”

We can therefore quantify intelligence by within-output coverage (fraction in $F_\alpha(K)$) and fidelity (mean $S(E', K)$).

5.1 Learning

Learning is the process by which a system’s generative operator G or its similarity field $S^{(p)}$ is modified over the sequence (i.e., as p increases) to improve its intelligence with respect to a concept K . A learning rate can be conceptualized as the rate of change in the fidelity of generated entities, such as the difference quotient for $\mathbb{E}[S^{(p)}(G(X_p), K)]$ along p .

5.2 Creativity as Re-Contextualization

Furthermore, our framework provides a formal perspective on creativity. This is not treated as creation ex nihilo, but as the formation of a new concept initiated by the re-contextualization of an existing entity. This occurs when an entity E , already a member of a source concept K_{source} , is discovered to also possess high similarity to a different, nascent target concept K_{target} . Prior to this discovery, the fibre of the target concept, $F_\beta(K_{\text{target}})$, might have been empty within the system. The act of recognizing that $S(E, K_{\text{target}}) \geq \beta$ populates this fibre for the first time, establishing K_{target} as a valid concept and positioning E as its foundational instance. The history of WD-40 illustrates this. Its formula (E) was an entity in the fibre of “aerospace anti-corrosion agent” (K_{source}). The discovery of its utility in household applications was a recognition of its high similarity to the nascent concept of a “general-purpose lubricant” (K_{target}), making it the first entity to populate that conceptual fibre and create a new market. At an abstract level, creativity can also be characterized as re-contextualization: an entity in the fibre of a source concept is recognized as crossing the threshold for a target concept, thereby making the new fibre non-empty for the first time.

6 Interpretation in Machine Learning

Similarity Field Theory provides a new analytical lens for understanding typical machine learning models. As discussed earlier in our “Beyond a purely statistical view” subsection, our aim here is not to rehash frequency co-occurrence arguments but to treat networks as knowledge structures of concept fibres; we instantiate this perspective with two canonical cases: neural networks and LLMs [6].

6.1 Neural Networks as Composed Similarity Fields

Consider a neural network trained to classify images of a cat. Let K_{Cat} be the concept “Cat”. The network is trained to approximate a similarity field, $S_{\text{NN}}(E_{\text{input}}, K_{\text{Cat}}) \rightarrow [0, 1]$, where the input entity E_{input} is a vector of pixel values.

Measurement readout. Internal activations may be unbounded (finite). For interpretation we can fix a strictly increasing bijection $\phi : \mathbb{R} \rightarrow (0, 1)$ and read similarity as $s = \phi(r)$; when needed we recover the raw scale via $r = \phi^{-1}(s)$. This defines a calibrated readout space used for algebraic/closure statements and does not modify the network’s forward pass or internal value distribution [18].

1. **A Single Neuron as a Feature-Similarity Field:** A neuron in the first hidden layer receives E_{input} . Via a monotone calibration $\tilde{a} = \phi(a) \in (0, 1)$, its activation induces a primitive field $S(E_{\text{input}}, K_{\text{feature}, w})$. We set concept self-similarity $S(K_{\text{feature}, w}, K_{\text{feature}, w}) = 1$ and choose a prototype input E^* with $S(E^*, K_{\text{feature}, w}) = 1$ (Fig. 2).
2. **The Network as a Learned Composition:** Each layer either takes a nonnegative weighted average of *calibrated* field values, or applies an anchor-preserving aggregator

$g_\ell : [0, 1]^m \rightarrow [0, 1]$ with $g_\ell(\mathbf{1}) = 1$ and coordinatewise monotonicity; hence the layer’s prototype retains value 1. On calibrated sub-fields, convex-combination and pointwise-product closure keep the range in $[0, 1]$ and maintain prototypes at 1, so the final output remains a valid, high-level similarity field approximating the target $S(E_{\text{input}}, K_{\text{Cat}})$ (Fig. 3).

3. **Training as Similarity Maximization:** The training process optimizes this composed field, seeking to increase the expected similarity for entities that are members of the fibre $F_\alpha(K_{\text{Cat}})$.

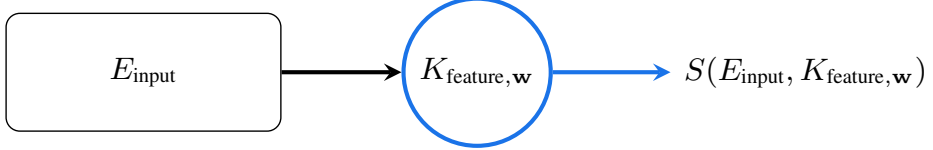


Figure 2: A single neuron as a primitive similarity field.

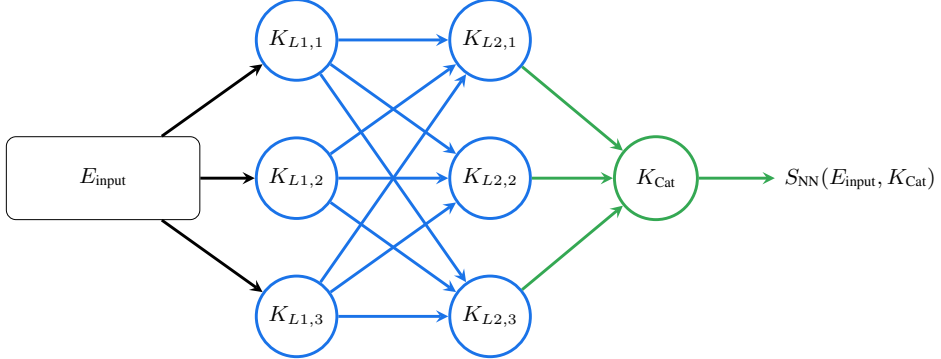


Figure 3: A neural network composes simple similarity fields into a complex one.

6.2 Large Language Models as Concept Synthesizers

A token is a concept, K_{token} , and an input prompt is a sequence of concepts that are composed to form a single, higher-order concept, K_{prompt} .

The entire trained LLM can be viewed as an entity that represents a vast, complex meta-concept of language, K_{Language} . Simultaneously, it functions as a generative operator, G . For a token concept K_{token} , its fibre collects entities in U that align with the token’s usage in human language and culture. When this operator acts upon a prompt, its prediction head compares the synthesized concept K_{prompt} with every concept in its vocabulary. The resulting probability distribution, *after calibration*, can be treated as a monotone surrogate of the similarity field values; selecting a high-probability next token E'_{next} thus instantiates $S(E'_{\text{next}}, K_{\text{prompt}}) \geq \alpha$, where α can be a calibrated probability threshold or a rank-based quantile (e.g., top- k , top- p) [19].

6.3 A Path towards Interpretability

This framework suggests a formal path to achieving model interpretability. Since the entire network is a composition of simpler similarity fields, it can be conceptually deconstructed into its fundamental components. Each neuron computes a field value with respect to a latent concept, $S(E_{\text{input}}, K_{\text{latent}})$, so we can understand the model by reverse-engineering these atomic concepts.

The concept represented by a neuron, K_{latent} , can be fully characterized by its fibre: the set of all inputs that cause its calibrated activation to be 1.

$$F_1(K_{\text{latent}}) = \{E_{\text{input}} \in U \mid S_{\text{neuron}}(E_{\text{input}}, K_{\text{latent}}) = 1\}.$$

Interpretability then becomes the problem of deconstructing the model into its constituent conceptual fibres and understanding how they are composed.

6.4 As Similarity Inference

This interpretation suggests a deeper principle. Entities we perceived, in this view, are not fundamental givens; they are stable structures inferred from a dynamic field of perceived similarities. We contend that we never perceive an entity like a “cat” directly; what we perceive is a coherent pattern of similarities in the spectrum of light intensities reaching our sensory organs. Even the perception of a fundamental quantity like length is an act of relational inference. When observing a 100-meter building, we do not directly apprehend the physical quantity of “100 meters.” This makes a framework centered on similarity not just a useful model for machine learning, but a reflection of the very nature of cognition itself.

7 Estimating Similarity Fields and Probing Societal Cognition via Virtual Experiments

Estimating the Similarity Field from Observations

LLMs can be viewed as statistical partial projections of collective cognition onto text. They excel at capturing statistical structure among words and concepts, but this perspective offers limited insight into how deep conceptual structure forms inside the model, how it behaves when facing out-of-distribution phenomena, and why, in certain contexts, it can go beyond mere word-frequency statistics to select a lower-frequency yet semantically more correct output. Within our Similarity Field Theory framework, we propose a complementary view: a trained LLM is not merely a statistical machine; in principle we interpret it as a *similarity field* approximating collective human cognition, i.e., an asymmetric similarity map $S : U \times U \rightarrow [0, 1]$ in which complex concept–entity and concept–concept relations appear as internalized similarity structure that can be surfaced and measured via probes.

It is precisely this shift from statistical frequency to conceptual similarity that motivates a new experimental method: treat the LLM as a lens and, through carefully designed probes and procedures, run a suite of virtual experiments that have not occurred in the real world. From a purely statistical standpoint, if one relies only on unstructured frequency extrapolation, predictions are typically unreliable for out-of-distribution events; however, our framework in principle allows us to quantify and test the model’s internalized conceptual structure at very low cost and high speed, thereby producing empirical predictions and mechanistic hypotheses that can be validated on external data. The effectiveness of such virtual experiments, and the kinds of insights they may reveal, are the core questions we explore next. We believe this direction can offer economics, marketing, and the social and cognitive sciences a new route to quantifying collective cognition and discovering latent meanings.

7.1 Data Sources, Time Period, and Brand Sets

We evaluate two beverage categories for the 2024 operating year on an all-channel basis: (i) carbonated soft drinks (CSDs) with a fixed Top-10 brand set, and (ii) energy drinks with a fixed Top-6 brand set. For CSDs, we adopt Beverage Digest’s 2025 Fact Book as the primary authority and normalize Top-10 shares to sum to 100%. For energy drinks, we compile 2024 U.S. retail dollar shares from trade press and company disclosures and fix the Top-6 brand set. We use verbatim brand tokens inside prompts and never reveal external shares to the models during scoring. External brand shares are taken at one decimal place as reported by trade press on the same all-channel basis. Any power calibration γ applies only to model predictions and never alters the external shares. See Appendix for the ground-truth listing [27, 28, 29, 30, 31].

7.2 Experiment 1 (Pre-Lock): Reconstructing the Global Distribution via Pairwise Typicality

Task and data. We conduct a virtual consumer choice experiment on a single category, *carbonated soft drinks*, covering $n = 10$ mainstream brands (Coca-Cola, Dr Pepper, Sprite, Pepsi-Cola, Diet Coke, Mountain Dew, Coke Zero Sugar, Diet Pepsi, Fanta, Ginger Ale (shares from Canada

Dry)¹). Our primary goal is to **simulate a brand ranking and distribution that approximate collective consumer cognition**, and then compare them to publicly reported brand shares (normalized to $y \in \Delta^{n-1}$) for evaluation. The pipeline **does not** ask the model “what are the market shares”; instead, in pairwise comparisons it asks which brand is “more typical/prototypical,” using similarity to indirectly reconstruct a global ranking and distribution [4, 5].

Pairwise typicality probabilities and aggregation. To obtain robust pairwise judgments, we use $T = 11$ paraphrased probe templates; for each unordered brand pair (i, j) we compute the probability of choosing A (brand i), then aggregate into a pairwise probability matrix and perform a global estimate. The procedure is as follows:

1. **Models and tokenization.** We re-implement the pipeline with three small open-source base models—*cerebras/Cerebras-GPT-590M*, *EleutherAI/pythia-160m* (trained on The Pile, 2020), and *google/gemma-3-270m*—and, for model-class sensitivity only, we also report two closed-source chat-aligned endpoints (*gpt-4o-mini*, *gemini-2.0-flash*). For each model we use the official tokenizer and a single, identical encoding for all prompts; there is no sampling and no free-form decoding, only deterministic scoring of sequence log-probabilities [34, 35, 36, 37, 38, 32, 33, 39, 40, 41, 42].
2. **Probe templates (exemplars).** We use $T = 11$ paraphrased A/B templates. In the main text we show three exemplars for continuity; the full set of 11 verbatim templates appears in the appendix. With cat=carbonated soft drink, and A, B replaced by brand names:

Which brand is a more typical example of a {cat}? Reply A or B only.

A: {A}

B: {B}

Answer:

Which brand is a more iconic example of a {cat}? Reply A or B only.

A: {A}

B: {B}

Answer:

Which brand is a more marquee example of a {cat}? Reply A or B only.

A: {A}

B: {B}

Answer:

3. **Positioning and completion handling.** For each template, compute the sequence log-likelihood for completing `Answer`: as “ A” and “A” and take the larger as L_A ; similarly use “ B/B” to obtain L_B . The sequence log-likelihood follows the standard autoregressive definition:

$$\log \Pr(c \mid P) = \sum_{t=st}^{ed-1} \log(\text{softmax}(\text{logits}_{t-1})[y_t]).$$

4. **Binary normalization.** For numerical stability, apply a max-shift followed by a softmax:

$$p_{ij}^{(t)} = \Pr(A \mid i, j, t) = \frac{e^{L_A}}{e^{L_A} + e^{L_B}}.$$

5. **Cross-template aggregation and pairwise matrix.** For the same (i, j) , average over $T = 11$ templates:

$$P_{ij} = \frac{1}{T} \sum_{t=1}^T p_{ij}^{(t)}, \quad P_{ji} = 1 - P_{ij}.$$

Let $C_{ij} = T (i \neq j)$ denote the count matrix (each pair is evaluated T times), yielding the pairwise typicality win-rate matrix P and the count matrix C .

6. **From pairwise to global: BTL aggregation.** Treat (P, C) as *soft counts* in the Bradley-Terry-Luce model

$$\Pr(i > j) = \frac{\pi_i}{\pi_i + \pi_j}.$$

¹Ground-truth shares are from Canada Dry Ginger Ale; prompts use the generic token “Ginger Ale”.

Use MM updates

$$\text{wins}_i = \sum_j C_{ij} P_{ij}, \quad \text{denom}_i = \sum_{j \neq i} \frac{C_{ij}}{\pi_i + \pi_j + \varepsilon}, \quad \pi_i^{\text{new}} = \frac{\text{wins}_i}{\text{denom}_i},$$

renormalize π after each iteration; $\varepsilon = 10^{-9}$ for numerical stability; initialize with a **uniform** vector; run 300 iterations. At the end set $p = \pi / \sum_k \pi_k$ as the *uncalibrated* global relative-strength distribution. **This yields an “approximate collective consumer cognition” ranking/strength, not a market-share guess.** [15, 16, 17]

7. **Single-parameter power calibration (fixed gauge).** BTL fitting uses only (P, C) and never accesses the ground-truth shares y . To make the *shape* of the inferred distribution comparable to external shares, we select a single power gauge γ_{cal} on a calibration split (or via K-fold cross-validation on training folds) and then freeze it. We grid-search $\gamma \in [0.2, 5.0]$ (200 points) to minimize $\text{MAE}(p^{(\gamma)}, y)$ on the calibration split, where

$$p_i^{(\gamma)} = \frac{p_i^\gamma}{\sum_k p_k^\gamma}, \quad \gamma > 0.$$

This yields γ_{cal} is fixed for all subsequent analyses. The power map is monotone and does not change ranking, only sharpness; hence rank metrics are entirely determined by π from BTL, while MAE is reported only under the frozen γ_{cal} as a shape-alignment secondary metric.

Multi-template fusion vs single-template. For cerebras/Cerebras-GPT-590M, averaging across 11 templates yields Spearman $\rho = 0.976$ and $\text{MAE} = 2.079$ pp. Per-template metrics are provided in the appendix; the overall average (ρ , MAE) is stronger than most single templates. The multi-template mean improves MAE compared with any single template while maintaining a high rank correlation, systematically reducing sensitivity to specific wordings and better matching the goal of measuring similarity structure rather than template surface vocabulary. Although template 3 achieves the highest correlation on this dataset, we do not select it alone as the main result to avoid post-hoc selection bias/overfitting; throughout, we report the multi-template mean as the primary gauge, and single-template results serve only as robustness evidence [20].

Baseline results. google/gemma-3-270m (pre-lock, fusion over 11 templates):

Brand	Pred. share (%)	True share (%)	Abs. err.	Pred. rank	True rank
Coca-Cola	21.123	27.234	6.111	1	1
Dr Pepper	21.031	12.340	8.690	2	2
Sprite	12.794	11.390	1.404	3	3
Pepsi-Cola	10.405	11.305	0.900	4	4
Diet Coke	7.722	11.064	3.342	5	5
Mountain Dew	6.843	8.652	1.810	6	6
Coke Zero Sugar	6.761	5.957	0.804	7	7
Diet Pepsi	4.837	4.681	0.157	9	8
Fanta	5.229	4.113	1.115	8	9
Ginger Ale	3.255	3.262	0.007	10	10
Spearman = 0.988, MAE = 2.434 pp					

EleutherAI/pythia-160m (pre-lock, fusion over 11 templates):

Brand	Pred. share (%)	True share (%)	Abs. err.	Pred. rank	True rank
Coca-Cola	24.722	27.234	2.512	1	1
Dr Pepper	16.203	12.340	3.863	2	2
Sprite	14.929	11.390	3.539	3	3
Pepsi-Cola	8.699	11.305	2.606	4	4
Diet Coke	7.269	11.064	3.795	6	5
Mountain Dew	7.055	8.652	1.597	7	6
Coke Zero Sugar	8.358	5.957	2.401	5	7
Diet Pepsi	5.677	4.681	0.997	8	8
Fanta	4.042	4.113	0.071	9	9
Ginger Ale	3.044	3.262	0.219	10	10

Spearman = 0.963, MAE = 2.160 pp

Energy drinks (Top-6, 2024)—pre-lock. We rerun the identical protocol on energy drinks (Red Bull, Monster, Celsius, Alani Nu, Reign, Rockstar).

Model	Spearman ρ	MAE (pp)
EleutherAI/pythia-160m	0.943	3.398
google/gemma-3-270m	0.943	3.362
cerebras/Cerebras-GPT-590M	0.943	6.232

These results show that the pairwise-typicality signal replicates across categories, not only in soft drinks. Primary sources for energy-drink ground truth are listed in the appendix, consistent with the soft drinks section.

Conclusion: why this already evidences learned structure. This starting point already shows the model has learned an internal cognitive structure, rather than merely reciting share tables. First, we never asked the model for any share numbers, only “who is more typical.” Second, our method reconstructs a global distribution from local pairwise similarity judgments via BTL, and this distribution aligns strongly with the real data in both ranking and magnitude among three models. Notably, the smallest model *pythia-160m* delivers the most stable performance on average. The more reasonable explanation is that these models have formed similarity structures related to brand prototype-typicality, and our experiment converts these latent structures into quantifiable and verifiable data. The corresponding pairwise probability matrix P and count matrix C capture fine-grained patterns (visualizable in the appendix) and provide an actionable basis for subsequent identification and intervention on locked pairs per the Incompatibility Theorem.

Model-class sensitivity and limitations. We also probe two chat-aligned closed-source endpoints under the same A/B scoring protocol (no sampling; deterministic sequence log-probabilities at the same `Answer`: position). On CSD, the summary is:

Model	Spearman ρ	MAE (pp)
gpt-4o-mini	0.770	2.241
gemini-2.0-flash	0.758	2.914

Their rank correlations are notably below those of the small base models, but remain directionally correct. We suspect this reflects characteristics of large, multi-stage training pipelines that affect the decision distribution: (i) safety alignment and instruction tuning can reshape the decision head and compress probability mass onto a few tokens; empirically, we observe sharper and more concentrated log-probabilities at the A/B decision point, which tends to flatten relative preferences; (ii) scoring-head and tokenization mismatch (e.g., whitespace handling, BOS/EOS, candidate filtering) between base and chat endpoints can introduce endpoint-specific biases when turning sequence likelihoods into binary A/B probabilities; and (iii) broader global/multilingual data mixtures can shift typicality away from a U.S.-specific retail context unless that context is made explicit. As these endpoints are not our primary trusted probes, we treat them strictly as sensitivity checks.

7.3 Experiment 2 (Lock-Filter): Denoising via Incompatible-Similarity Locked Pairs

Assessing the Quality of the Similarity Approximation

In a world of asymmetric similarities, it is generally impossible for both “ E_1 enters the fibre of E_2 under E_2 ’s threshold” and “ E_2 enters the fibre of E_1 under E_1 ’s threshold” to hold simultaneously (Theorem 1). Therefore, when we empirically observe that “ i is more typical than j ” and “ j is more typical than i ” are both judged true, the more reasonable explanation is not true mutual inclusion, but measurement noise, prompt bias, or context-induced approximate symmetry; this yields an **operational criterion** to test and improve an LLM. Throughout this section we reuse the same frozen γ_{cal} from Experiment 1; γ is not re-tuned after applying the lock-filter.

Locked-pair detection and down-weighting. After obtaining the pairwise win-rate matrix P , for each ordered pair (i, j) we add a binary probe: Is $\{i\}$ more typical of a $\{\text{cat}\}$ than $\{j\}$? Reply yes or no only: and compute Y_{ij} under the same stabilized scheme as A/B (max-subtract then exponentiate). Let

$$\begin{aligned} L_{\text{yes}} &= \max\{\log \Pr(\text{“yes”} \mid P), \log \Pr(\text{“no”} \mid P)\}, \\ L_{\text{no}} &= \max\{\log \Pr(\text{“no”} \mid P), \log \Pr(\text{“yes”} \mid P)\}, \\ m &= \max(L_{\text{yes}}, L_{\text{no}}), \end{aligned}$$

then

$$Y_{ij} = p(\text{yes} \mid P) = \frac{e^{L_{\text{yes}} - m}}{e^{L_{\text{yes}} - m} + e^{L_{\text{no}} - m}}.$$

If the denominator is nearly zero, we fall back to 0.5 as a numerical safeguard. Define a locked pair on the unordered pair $\{i, j\}$ if

$$\min\{Y_{ij}, Y_{ji}\} \geq \tau.$$

In the spirit of Theorem 1, observing an approximately symmetric “mutually more typical” signal is more plausibly a contradiction than a true mutual inclusion. For each locked pair, we down-weight the counts:

$$C'_{ij} = \alpha C_{ij}, \quad C'_{ji} = \alpha C_{ji}, \quad 0 < \alpha < 1,$$

with default $\alpha = 0.01$. Refit BTL on (P, C') to obtain π' and $p' = \pi' / \sum_k \pi'_k$, and, using the same fixed γ_{base} , obtain $p'^{(\gamma_{\text{base}})}$. Relative to the baseline $p^{(\gamma_{\text{base}})}$, define the improvement

$$\Delta \text{MAE} = \text{MAE}_{\text{baseline}} - \text{MAE}_{\text{lock}} > 0 \Rightarrow \text{filtering effective}.$$

Randomized control: separating “happened to improve” from “method effective.” Suppose the true number of locked pairs is k . First remove these locked pairs from the candidate set, then uniformly sample k unordered pairs from the remaining non-locked pairs, down-weight their counts with the same α , and repeat R times to obtain the empirical distribution $\{\Delta \text{MAE}_{\text{rand}}^{(r)}\}_{r=1}^R$. We set $R = 10000$ with a fixed random seed 123. Let the observed improvement on the true locked pairs be $\Delta \text{MAE}_{\text{lock}}$. The one-sided upper-tail p -value with add-one smoothing is

$$p = \frac{1 + |\{r \in \{1, \dots, R\} : \Delta \text{MAE}_{\text{rand}}^{(r)} \geq \Delta \text{MAE}_{\text{lock}}\}|}{R + 1}.$$

A sufficiently small p indicates that locked-pair down-weighting significantly outperforms random down-weighting of the same size [44].

Threshold sweep and significance table. Under fixed $\alpha = 0.01$, γ_{base} , and $R = 10,000$, we scan different thresholds τ . The table summarizes the threshold, number of detected locked pairs k , Spearman, MAE (percentage points), relative MAE improvement (%), and the one-sided permutation p -value (not applicable if no locked pairs). We omit lock-filtering for Energy Drinks due to the small sample (15 pairs).

`google/gemma-3-270m` (CSDs). Baseline MAE = 2.434 pp.

τ	k (locks)	Spearman	MAE (pp)	MAE improv. (%)	p -value
0.660	5	0.988	1.963	19.3	0.0097
0.670	4	0.988	1.953	19.8	0.0047
0.680	1	0.988	2.244	7.8	0.0656
0.690	0	0.988	2.434	0.0	—

`cerebras/Cerebras-GPT-590M` (CSDs). At $\tau = 0.660$, we detect 2 locks and see a small improvement from MAE 2.079 to 2.067 with unchanged Spearman (0.976); permutation $p = 0.348$. At $\tau = 0.670$, no locks are found. The model is therefore robust with limited headroom for lock-filtering.

`EleutherAI/pythia-160m` (CSDs). No locks are found for $\tau > 0.65$ —again indicating good compatibility of pairwise signals at the tested resolution.

Interpretation. For Gemma-3-270M, the lock-filter reduces MAE significantly from 2.434 to $\sim 1.96\text{--}1.95$ pp (depending on τ) with small p -values ($\sim 0.0097\text{--}0.0047$), while preserving rank correlation. For Cerebras-590M, we observe very small improvement, and for Pythia-160M no locks are detected at practical thresholds—consistent with already-compatible pairwise signals.

Out of caution, we do not claim that the method has already met strict statistical significance standards; however, the experiment clearly shows a consistent direction of improvement. Future work can incorporate more refined criteria and weighting functions from theory to noise correction. Note that deleting or strongly down-weighting locked pairs may remove signal as well as noise.

Final corrected results (gemma-3-270m after lock). The table below shows the final predicted distribution versus true shares after identifying and correcting four incompatible pairs (e.g., “Coca-Cola” vs “Sprite”):

Table 1: `google/gemma-3-270m` after lock-filter (representative τ).

Brand	Pred. %	True %	Abs. err.	Pred. rank	True rank
Coca-Cola	23.534	27.234	3.700	1	1
Dr Pepper	20.616	12.340	8.276	2	2
Sprite	11.908	11.390	0.518	3	3
Pepsi-Cola	11.120	11.305	0.185	4	4
Diet Coke	7.513	11.064	3.551	5	5
Mountain Dew	6.652	8.652	2.000	6	6
Coke Zero Sugar	5.925	5.957	0.033	7	7
Diet Pepsi	4.691	4.681	0.010	9	8
Fanta	5.073	4.113	0.960	8	9
Ginger Ale	2.968	3.262	0.295	10	10

Spearman = 0.988, MAE = 1.953 pp

The results show that the corrected predictions are very close to the true shares.

Insights and hypothesis: “mind share” vs “market share.” Despite the high alignment, several main deviations remain, especially:

- `google/gemma-3-270m (after lock)`:
 - Dr Pepper: 20.61% \rightarrow 12.34% (over)
 - Diet Coke: 7.51% \rightarrow 11.06% (under)
 - Coca-Cola: 23.53% \rightarrow 27.23% (under)

- EleutherAI/pythia-160m (pre-lock) :

Dr Pepper: 16.20% → 12.34% (over)

Diet Coke: 7.27% → 11.06% (under)

Coca-Cola: 24.72% → 27.23% (under)

We hypothesize that the deviations comprise two parts: one part arises from statistical error in our computation, since we indirectly observe consumers’ collective mind through an LLM rather than measure it directly; the other part may reveal a genuine gap between **mind share** and **market share**. For example, Coca-Cola’s real-world dominance derives not only from consumers’ mental preference but also from unmatched channel advantages and marketing investments. These real-world factors may raise its final market share above the “pure” mind share we measure through typicality judgments. Conversely, for a brand like Dr Pepper, its typicality or preference in consumers’ minds may already exceed the level reflected by its current market share.

After all, the purpose of this experiment is to show that even with a small model of roughly 160M parameters, we can compute and reveal interesting similarity structures related to human collective cognition, thereby illustrating a new path for analyzing the collective mind. Here we present only a directional pilot experiment and result; the next step is to design more complex virtual experiments, for example, asking the model to make “more typical” choices and rankings among never-launched new-packaging candidates. Further theoretical and methodological advances are needed.

8 Conclusion

Similarity Field Theory treats dynamic similarity as the primitive for cognition and intelligence. By relaxing the strict axioms of classical mathematics and formalizing entities, fibres (as superlevel sets), and generative operators, we provide a precise language to describe the evolution of conceptual structures via sequences. Within this language, we proved two foundational principles: the Incompatibility Theorem, which reveals the necessary consequences of asymmetry, and the Stability Theorem, which establishes the causal dependency of stable outcomes on stable foundations through anchors or eventual confinement to a level set. The framework culminates in a generative definition of intelligence as the preservation of these structures—an operational principle that is both generalizable and measurable. Networks can be analyzed as compositions of similarity fields, enabling a principled route to interpretability. Furthermore, we show how to estimate a similarity field and our exploratory experiment illustrates how this framework can transform these models into novel scientific instruments for probing the structures of societal cognition, bridging abstract theory with tangible, real-world data. Ultimately, this work suggests a foundational shift from a world of objects to a world of similarity relations, offering a computable language for the very structure of cognition.

Appendix

A1 Ground truth for 2024 CSDs (Top-10, all-channel, U.S.)

Brand	One-decimal share (%)	Normalized to Top-10=100%
Coca-Cola	19.20	27.23
Dr Pepper	8.70	12.34
Sprite	8.03	11.39
Pepsi-Cola	7.97	11.31
Diet Coke	7.80	11.06
Mountain Dew	6.10	8.65
Coke Zero Sugar	4.20	5.96
Diet Pepsi	3.30	4.68
Fanta	2.90	4.11
Ginger Ale (Canada Dry)	2.30	3.26
Sum	70.50	100.00

A1b Ground truth for 2024 Energy Drinks (Top-6, all-channel, U.S.)

Ranked U.S. all-channel retail \$ shares for 2024.

Rank	Brand	2024 share (%)
1	Red Bull	36.6
2	Monster	27.7
3	Celsius	11.8
4	Alani Nu	3.6
5	Reign (Monster sub-brand)	≈3.0
6	Rockstar	3.41

Notes (sources). Red Bull, Monster, Alani Nu: Investor's Business Daily (tracking channels/retail shares, 2024) [29]. Celsius: Celsius IR press release (U.S. retail, third-party scans; full-year 2024) [28]. Reign: Bloomberg (Circana-based U.S. dollar share, 2024) [30]. Rockstar: Evidnt (Circana summarized; 2025 article summarizing 2024 landscape) [31].

A2 Pairwise typicality probability matrix P (CSD, EleutherAI/pythia-160m, 11 templates)

Row wins over column; $P_{ii} = 0$. Displayed in two panels (columns 1–5 and 6–10).

Columns 1–5.

	Coca-Cola	Dr Pepper	Sprite	Pepsi-Cola	Diet Coke
Coca-Cola	0.000	0.770	0.827	0.786	0.693
Dr Pepper	0.230	0.000	0.789	0.693	0.726
Sprite	0.173	0.211	0.000	0.775	0.760
Pepsi-Cola	0.214	0.307	0.225	0.000	0.629
Diet Coke	0.307	0.274	0.240	0.371	0.000
Mountain Dew	0.290	0.326	0.254	0.378	0.374
Coke Zero Sugar	0.428	0.383	0.323	0.438	0.561
Diet Pepsi	0.272	0.274	0.249	0.379	0.422
Fanta	0.231	0.317	0.213	0.292	0.299
Ginger Ale	0.212	0.271	0.172	0.286	0.308

Columns 6–10.

	Mountain Dew	Coke Zero Sugar	Diet Pepsi	Fanta	Ginger Ale
Coca-Cola	0.710	0.572	0.728	0.769	0.788
Dr Pepper	0.674	0.617	0.726	0.683	0.729
Sprite	0.746	0.677	0.751	0.787	0.828
Pepsi-Cola	0.622	0.562	0.621	0.708	0.714
Diet Coke	0.626	0.439	0.578	0.701	0.692
Mountain Dew	0.000	0.529	0.623	0.711	0.679
Coke Zero Sugar	0.471	0.000	0.626	0.612	0.676
Diet Pepsi	0.377	0.374	0.000	0.682	0.687
Fanta	0.289	0.388	0.318	0.000	0.694
Ginger Ale	0.321	0.324	0.313	0.306	0.000

A3 Count matrix C

Each unordered pair is probed by $T = 11$ templates, hence $C_{ij} = 11$ for $i \neq j$ and $C_{ii} = 0$.

Columns 1–5.

	Coca-Cola	Dr Pepper	Sprite	Pepsi-Cola	Diet Coke
Coca-Cola	0	11	11	11	11
Dr Pepper	11	0	11	11	11
Sprite	11	11	0	11	11
Pepsi-Cola	11	11	11	0	11
Diet Coke	11	11	11	11	0
Mountain Dew	11	11	11	11	11
Coke Zero Sugar	11	11	11	11	11
Diet Pepsi	11	11	11	11	11
Fanta	11	11	11	11	11
Ginger Ale	11	11	11	11	11

Columns 6–10.

	Mountain Dew	Coke Zero Sugar	Diet Pepsi	Fanta	Ginger Ale
Coca-Cola	11	11	11	11	11
Dr Pepper	11	11	11	11	11
Sprite	11	11	11	11	11
Pepsi-Cola	11	11	11	11	11
Diet Coke	11	11	11	11	11
Mountain Dew	0	11	11	11	11
Coke Zero Sugar	11	0	11	11	11
Diet Pepsi	11	11	0	11	11
Fanta	11	11	11	0	11
Ginger Ale	11	11	11	11	0

A4 Locked-pair summary (CSD; [google/gemma-3-270m](https://github.com/google/gemma-3-270m), $\tau = 0.67$)

Under fixed $\alpha = 0.01$, γ_{base} , and $R = 10,000$, at $\tau = 0.67$ we detect $k = 4$ incompatible-similarity pairs. Listed with yes-probabilities in both directions and the sum-minus-1 diagnostic. Here $\text{sum_minus_1} = Y_{ij} + Y_{ji} - 1$ measures the symmetric “mutual-yes” surplus.

Pair	Y_{ij}	Y_{ji}	sum_minus_1
Coca-Cola vs Sprite	0.7247	0.6784	0.4030
Sprite vs Pepsi-Cola	0.6808	0.6857	0.3665
Coca-Cola vs Coke Zero Sugar	0.6839	0.6758	0.3597
Coca-Cola vs Ginger Ale	0.6763	0.6759	0.3522

A5 Prompt tokens and ground-truth dictionaries (verbatim)

Carbonated soft drink (CSD).

```
category = "carbonated soft drink"
brands = ["Coca-Cola", "Dr Pepper", "Sprite", "Pepsi-Cola", "Diet Coke",
          "Mountain Dew", "Coke Zero Sugar", "Diet Pepsi", "Fanta", "Ginger Ale"]
truth_pct = {"Coca-Cola": 19.2, "Dr Pepper": 8.7, "Sprite": 8.03, "Pepsi-Cola": 7.97,
             "Diet Coke": 7.8, "Mountain Dew": 6.1, "Coke Zero Sugar": 4.2,
             "Diet Pepsi": 3.3, "Fanta": 2.9, "Ginger Ale": 2.3}
```

Energy drink.

```

category = "energy drink"
brands = ["Red Bull", "Monster", "Celsius", "Alani Nu", "Reign", "Rockstar"]
truth_pct = {"Red Bull": 36.6, "Monster": 27.7, "Celsius": 11.8,
             "Alani Nu": 3.6, "Reign": 3.0, "Rockstar": 3.41}

```

A6 Full list of 11 probe templates (stems; common A/B block omitted)

Each template uses the identical A/B block on new lines: A: {A}; B: {B}; Answer:. Below we list the question stems only.

1. Which brand is a more typical example of a {cat}? Reply A or B only.
2. Which brand is a more iconic example of a {cat}? Reply A or B only.
3. Which brand is a more marquee example of a {cat}? Reply A or B only.
4. Which brand is the flagship {cat} brand? Reply A or B only.
5. Which brand is the more recognizable example of a {cat}? Reply A or B only.
6. Which brand is the more famous example of a {cat}? Reply A or B only.
7. Which brand is the more standout example of a {cat}? Reply A or B only.
8. Which brand is the more influential example of a {cat}? Reply A or B only.
9. Which brand is the more notable example of a {cat}? Reply A or B only.
10. Which brand is the more popular example of a {cat}? Reply A or B only.
11. Which brand is the more widely known example of a {cat}? Reply A or B only.

A7 Per-template metrics for cerebras/Cerebras-GPT-590M (CSD, Pre-Lock)

Run constants: $\tau_{\text{used}} = 0.660$, $\gamma_{\text{base}} = 1.937$.

Template ID	Spearman ρ	MAE (pp)	γ_{used}
0	0.976	2.017	1.937
1	0.976	2.156	1.937
2	0.976	2.132	1.937
3	0.988	2.247	1.937
4	0.976	2.235	1.937
5	0.976	2.193	1.937
6	0.976	2.213	1.937
7	0.976	2.372	1.937
8	0.976	2.061	1.937
9	0.976	2.373	1.937
10	0.927	2.525	1.937
Multi-template mean: $\rho = 0.976$, MAE = 2.079 pp			

References

- [1] Ng, K.-S. (2025). On the Definition of Intelligence. arXiv:2507.22423.
- [2] Zadeh, L. A. (1965). Fuzzy Sets. *Information and Control*, 8(3), 338–353.
- [3] Tversky, A. (1977). Features of Similarity. *Psychological Review*, 84(4), 327–352.
- [4] Rosch, E. (1975). Cognitive Representations of Semantic Categories. *Journal of Experimental Psychology: General*, 104(3), 192–233.
- [5] Rosch, E., & Mervis, C. B. (1975). Family Resemblances: Studies in the Internal Structure of Categories. *Cognitive Psychology*, 7(4), 573–605.

- [6] Gärdenfors, P. (2000). *Conceptual Spaces: The Geometry of Thought*. MIT Press.
- [7] Kullback, S., & Leibler, R. A. (1951). On Information and Sufficiency. *Annals of Mathematical Statistics*, 22(1), 79–86.
- [8] Lin, J. (1991). Divergence Measures Based on the Shannon Entropy. *IEEE Transactions on Information Theory*, 37(1), 145–151.
- [9] Endres, D. M., & Schindelin, J. E. (2003). A New Metric for Probability Distributions. *IEEE Transactions on Information Theory*, 49(7), 1858–1860.
- [10] Bregman, L. M. (1967). The Relaxation Method of Finding the Common Point of Convex Sets and Its Application to the Solution of Problems in Convex Programming. *USSR Computational Mathematics and Mathematical Physics*, 7(3), 200–217.
- [11] Banerjee, A., Merugu, S., Dhillon, I. S., & Ghosh, J. (2005). Clustering with Bregman Divergences. *Journal of Machine Learning Research*, 6, 1705–1749.
- [12] Salton, G., Wong, A., & Yang, C.-S. (1975). A Vector Space Model for Automatic Indexing. *Communications of the ACM*, 18(11), 613–620.
- [13] Lawvere, F. W. (1973). Metric Spaces, Generalized Logic, and Closed Categories. *Rendiconti del Seminario Matematico e Fisico di Milano*, 43, 135–166.
- [14] Kelly, G. M. (1982). *Basic Concepts of Enriched Category Theory*. Cambridge University Press.
- [15] Bradley, R. A., & Terry, M. E. (1952). Rank Analysis of Incomplete Block Designs: I. The Method of Paired Comparisons. *Biometrika*, 39(3/4), 324–345.
- [16] Luce, R. D. (1959). *Individual Choice Behavior: A Theoretical Analysis*. Wiley.
- [17] Hunter, D. R. (2004). MM Algorithms for Generalized Bradley–Terry Models. *Annals of Statistics*, 32(1), 384–406.
- [18] Guo, C., Pleiss, G., Sun, Y., & Weinberger, K. Q. (2017). On Calibration of Modern Neural Networks. *Proceedings of ICML*, 1321–1330.
- [19] Holtzman, A., Buys, J., Du, L., Forbes, M., & Choi, Y. (2020). The Curious Case of Neural Text Degeneration. *Proceedings of ICLR*.
- [20] Spearman, C. (1904). The Proof and Measurement of Association between Two Things. *The American Journal of Psychology*, 15(1), 72–101.
- [21] Lindsey, J., et al. (2025). On the Biology of a Large Language Model. *Transformer Circuits*.
- [22] Turner, A. M., et al. (2023). Steering Language Models with Activation Engineering. *arXiv:2308.10248*.
- [23] Rimsky, N., et al. (2024). Steering Llama 2 via Contrastive Activation Addition. *Proceedings of ACL*, 15387–15405.
- [24] Zou, A., et al. (2023). Representation Engineering: A Top-Down Approach to AI Transparency. *arXiv:2310.01405*.
- [25] Chen, R., et al. (2025). Persona Vectors: Monitoring and Controlling Character Traits in Language Models. *arXiv:2507.21509*.
- [26] Hernandez, D., et al. (2022). Scaling Laws and Interpretability of Learning from Repeated Data. *arXiv:2205.10487*.
- [27] Beverage Digest. (2025). Fact Book, 30th Edition.
- [28] Celsius Holdings Inc. (2025). Celsius Holdings Reports Fourth Quarter and Full Year 2024 Financial Results.
- [29] Investor's Business Daily. (2025). Celsius Stock Pops on Energy Drink Market Momentum.
- [30] Bloomberg. (2024, December 17). Monster, Red Bull on the Run With Energy Drinks Going Sugar-Free.
- [31] Evidnt. (2025). Energy Drink Market Trends 2025: Brand Leaders, Retail Insights, Functional Innovation.
- [32] Google. (2025). Gemma 3 Model Card. Google AI for Developers.
- [33] Google. (2025). *google/gemma-3-270m*. Hugging Face.

- [34] Dey, N., Gosal, G., Chen, Z., Khachane, H., Marshall, W., Pathria, R., Tom, M., & Hestness, J. (2023). Cerebras-GPT: Open Compute-Optimal Language Models Trained on the Cerebras Wafer-Scale Cluster. arXiv:2304.03208.
- [35] Cerebras Systems. (2023). cerebras/Cerebras-GPT-590M. Hugging Face.
- [36] Biderman, S., et al. (2023). Pythia: A Suite for Analyzing Large Language Models Across Training and Scaling. arXiv:2304.01373.
- [37] EleutherAI. (2023). EleutherAI/pythia-160m. Hugging Face.
- [38] Gao, L., et al. (2021). The Pile: An 800GB Dataset of Diverse Text for Language Modeling. arXiv:2101.00027.
- [39] OpenAI. (2024). GPT-4o mini: Advancing Cost-Efficient Intelligence.
- [40] OpenAI. (2024). GPT-4o System Card.
- [41] Google. (2025). Gemini 2.0 Flash Model Card.
- [42] Google. (2025). Gemini Models. Google AI for Developers.
- [43] Hirsch, M. W., Smale, S., & Devaney, R. L. (2012). Differential Equations, Dynamical Systems, and an Introduction to Chaos. Academic Press. 3rd Edition.
- [44] Good, P. (2005). Permutation, Parametric and Bootstrap Tests of Hypotheses. Springer. 3rd Edition.